

다공성 막을 포함하는 미세유체칩을 이용한 항암 지질나노입자 연속 생산 공정

오도현*** · 한수경*** · 류영현*** · 안국영*** · 최인성*** · 최성욱***†^{ORCID}

*가톨릭대학교 바이오메디컬화학공학과, **가톨릭대학교 생명공학과
(2022년 3월 10일 접수, 2022년 6월 30일 수정, 2022년 8월 8일 채택)

Fabrication of Microfluidic Chips Containing Porous Membrane for Continuous Production of Lipid Nanoparticles

Do-Hyun Oh***, Soo Kyung Han***, Young-Hyun Ryu***,
Guk-Young Ahn***, Inseong Choi***, and Sung-Wook Choi***†^{ORCID}

*Biomedical and Chemical Engineering, The Catholic University of Korea, 43 Jibong-ro,
Wonmi-gu, Bucheon-si, Gyeonggi-do, Korea

**Department of Biotechnology, The Catholic University of Korea, 43 Jibong-ro, Wonmi-gu, Bucheon-si, Gyeonggi-do, Korea
(Received March 10, 2022; Revised June 30, 2022; Accepted August 8, 2022)

초록: 다공성 막을 중간층으로 갖는 폴리디메틸실록산 미세유체칩을 이용하여 항암 약물인 독소루비신을 함유한 지질나노입자를 연속적인 공정으로 제조하였다. 불연속상으로는 지질, 독소루비신, 및 라우릭 산을 함유한 에탄올상을, 연속상으로는 증류수를 각각 시린지펌프를 이용하여 미세유체칩에 투입하였다. 작은 기공을 갖는 다공성막을 사용하고, 연속상의 유속이 높을 수록 작은 지질나노입자가 제조되었다. 라우릭 산은 지질나노입자의 콜로이드 안정성을 증가시켜 주었고, 독소루비신과 라우릭 산의 첨가는 HeLa 암세포주에서 높은 세포 독성을 나타내었다. 이러한 미세유체칩은 다른 약물은 물론, mRNA와 siRNA를 함유한 지질나노입자제조에 응용될 수 있다.

Abstract: A polydimethylsiloxane (PDMS) microfluidic device containing a porous membrane as a middle layer was fabricated to continuously produce lipid nanoparticles (LNPs). Ethanol with lipids and water were used as discontinuous and continuous phases. Doxorubicin and lauric acid were added in the ethanol phase for tumor therapy and LNP stability. The smaller LNPs were prepared at the higher flow rate of the continuous phase by using the membrane with smaller pore size. The LNPs with a size of 87.6 ± 3.84 nm were obtained at 0.3 mL/min of the flow rate of the continuous phase by using the membrane with a pore size of 0.02 μ m. The addition of lauric acid enhanced the colloidal stability of LNPs. In addition, the LNPs with doxorubicin and lauric acid exhibited lower viability for HeLa cells and enhanced colloidal stability of LNPs. The microfluidic device with a porous membrane can be used as a general platform for the continuous production of LNPs containing mRNA, siRNA, and other therapeutic agents.

Keywords: microfluidic, porous membrane, lipid nanoparticle, tumor therapy.

Introduction

Recently, lipid nanoparticles (LNPs) have attracted much attention as delivery nanovesicles for therapeutic agents and RNAs.¹⁻⁴ The delivery system based on LNPs includes many advantages such as excellent biocompatibility, low toxicity, and high delivery efficiency.^{5,6} In addition, LNP can encapsulate both hydrophobic and hydrophilic therapeutic agents at

the core and lipid layer.⁷ These features of LNP allow for wide applications in cosmetics, bioimaging, and tissue engineering.⁸⁻¹⁰

There are a variety of techniques for the production of LNPs, including film hydration, extrusion, microfluidic device, and so on.¹¹⁻¹³ Among them, microfluidic-based techniques were often applied for the continuous and large-scale production of LNPs. This approach has many advantages of miniaturization, low reagent consumption, high reproducibility, and low required energy.¹⁴ However, most methods for the fabrication of microfluidic devices were mainly limited to soft lithography.^{15,16} Although soft lithography is a well-developed and versatile technique, multiple and complex procedures with expensive

†To whom correspondence should be addressed.
choisw@catholic.ac.kr, ORCID[®] 0000-0002-5075-8798
©2022 The Polymer Society of Korea. All rights reserved.

equipment are pointed out as a major hurdle for device fabrication. There is a need for an easy and simple method for device fabrication applicable to nanovesicle production.

In this work, we developed a simple method of the fabrication of a polydimethylsiloxane (PDMS) microfluidic device and demonstrated the continuous production of LNPs with doxorubicin. The feature of our approach is the employment of a porous membrane in the microfluidic device. The flow channels for inlets and outlet were prepared by using a 3D printing and temporary method. The size of LNPs with less than 100 nm could be continuously obtained using the microfluidic device with a porous membrane. We believe that our microfluidic device has great potential as a general platform for the high throughput and continuous production of LNPs.

Experimental

Materials. All chemicals were obtained from Sigma-Aldrich and used as received unless otherwise specified. Poly(ϵ -caprolactone) (PCL, $M_w=14000$) was used to fabricate the 3D-printed pattern. Dichloromethane (DCM) was used as an organic solvent to remove the PCL channel selectively. Polydimethylsiloxane (PDMS) elastomer and curing agent (Sylgard 184) were purchased from Sewang Hitech (Gimpo, Korea). Dulbecco's phosphate-buffered saline (DPBS) and Dulbecco's modified Eagle's medium (DMEM) were purchased from WELGENE Inc. (Gyeongsan, Korea). The culture medium consisted of Dulbecco's modified Eagle's medium (DMEM) supplemented with 10% fetal bovine serum (FBS) and 1% antibiotics (containing penicillin and streptomycin). Cell Counting Kit-8 (CCK-8, Dojindo Co., Ltd., Tokyo, Japan) was used to quantitatively measure cell numbers. 1,2-Dipalmitoyl-sn-glycero-3-phosphocholine (DPPC, Avanti Polar Lipids, INC.), cholesterol (Avanti Polar Lipids, INC.), dodecanoic acid (Lauric acid, LA, 98%), doxorubicin hydrochloride salt was purchased from LC Laboratories (Woburn, USA). Cellulose acetate membrane filter (0.80 μm pore size, ADVANTEC, Japan), polytetrafluoroethylene membrane (0.45 μm pore size, GVS Filter Technology, USA). Anodisc filter (0.02 μm pore size, cytiva, Germany), cellulose dialysis membranes (MWCO 12-14 kDa) were purchased from Cellu-Sep (Sequin, TX, USA).

Fabrication of Microfluidic Chips. The PCL pattern as a template of the top and bottom PDMS layers was printed on a Petri dish from a nozzle heated to 70 °C using a 3D printer (EZ-Robo GX, Iwashita Engineering Inc., Japan). The Petri

dish of the PCL pattern was placed and the PDMS mixture (PDMS elastomer and curing agent, a weight ratio of 10:1) was poured into the dish. After degassing for 60 min, the Petri dish was placed in an oven at 40 °C for 12 h. The cured PDMS was removed from the Petri dish and immersed in DCM to dissolve the 3D printed PCL pattern. The PDMS layer was then dried at room temperature for DCM evaporation. Two PDMS layers and a membrane were assembled and fixed between two acrylic plates using screws. After drilling, the inlet/outlet channels were connected to a syringe pump (NE-1000, New Era Pump Systems Inc., NY, USA) using L connectors (1/16 in. ID \times 3/32 in. OD) and Tygon[®] tubing (1/32 in. ID \times 3/32 in. OD). The morphology of the inlet/outlet channels and microfiber channels was observed using a scanning electron microscope (SEM, S-4800, Hitachi, Tokyo, Japan).

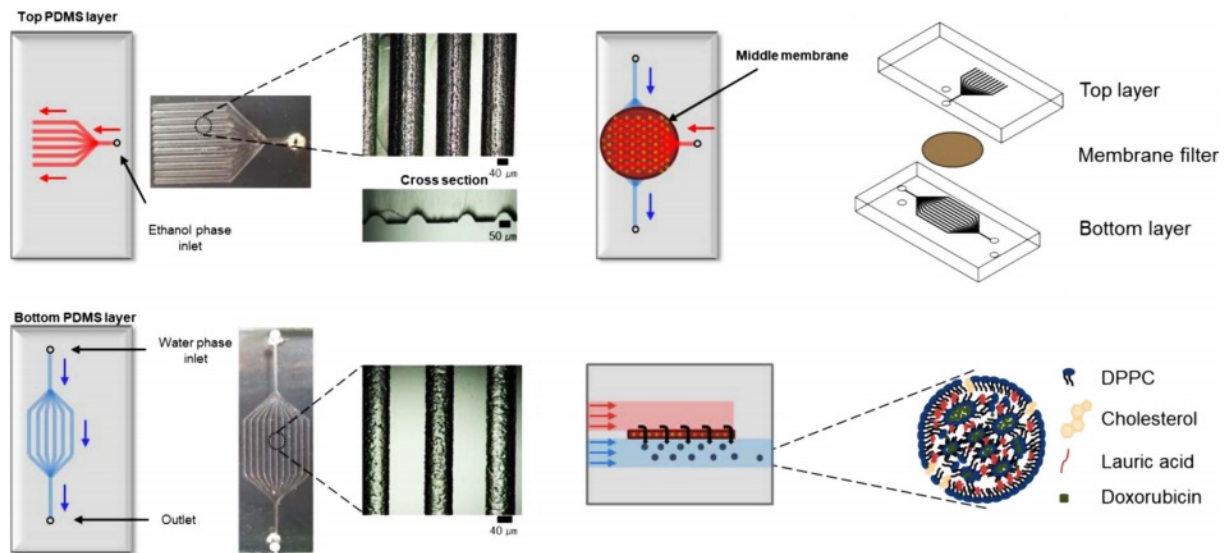
Production of Lipid Nanoparticles. The ethanol phase containing DOX, DPPC, cholesterol, and LA was used as the discontinuous phase and D.W. was used as the continuous phase. The basic recipe for LNPs was 20 mg of DPPC and 10 mg of cholesterol in ethanol (10 mL). LA (7.5 mg) or DOX (2.6 mg) were added into the ethanol phase (Table 1). The flow rate of the continuous phase was varied as 0.1, 0.2, and 0.3 mL/min, where the flow rate of the discontinuous phase was maintained at 0.01 mL/min. The product was placed in a vial and gently stirred for 1 day to evaporate the remaining ethanol. Drugs not loaded into the LNP were then removed by dialysis. Droplet and sphere sizes were analyzed using dynamic light scattering (DLS, Zetasizer Nano ZS, Malvern Instruments, Malvern, UK).

Stability Study. Stability studies were performed on drug-free LNP formulations with and without LA. LNPs were stored for 10 weeks under static conditions at room temperature.

Antitumoral Effect. NIH/3T3 and HeLa cell lines (Korea Cell Line Bank, Seoul, Korea) were used as model cells to evaluate cell viability. Each cell line was seeded in 96-well plates at a density of 1×10^4 cells per well, and the use of

Table 1. Recipe of CON, LA, DOX, and DOX-LA

Name	Ethanol (mL)	DOX (mg)	DPPC (mg)	Cholesterol (mg)	LA (mg)
CON	10.0	-	20.0	10.0	-
LA	10.0	-	20.0	10.0	7.5
DOX	10.0	2.60	20.0	10.0	-
DOX-LA	10.0	2.60	20.0	10.0	7.5



Scheme 1. Schematic illustration of the procedure for the microfluidic device fabrication.

DMEM containing 10% FBS and 1% antibiotics (penicillin and streptomycin) at 37 °C, 5% CO₂ atmosphere 24 h. After 24 h, each well was washed three times with DPBS to remove the medium, and then four types of LNPs were added to the wells containing each cell line. After 24 h, each well was washed three times with DPBS to remove the LNPs, and then CCK solution that was 50-fold diluted with free media was added to the wells. After 2 h, the number of cells was measured at a wavelength of 450 nm using a microplate reader (Infinite F50, Tecan).

Results and Discussion

Fabrication and Characterization of Chip. Scheme 1 shows schematics of the chip fabrication and photograph/SEM images of the PDMS layer, respectively. The chip consists of two PDMS layers and one membrane. The upper layer has an ethanol inlet channel, the middle layer has a membrane, and the bottom layer has a water inlet and production outlet. The

top and bottom PDMS layers were prepared using a 3D printed PCL pattern as a template. The inlet channel was split into eleven branched channels. All the channels had a semicircular shape. We developed the branched channels to introduce the ethanol phase throughout the membrane at the same time.¹⁷ The ethanol channel was 740 μm in width and 100 μm in depth, and the water channel was 427 μm in width and 230 μm in depth. The middle layer was prepared using a membrane having a pore size of 0.80, 0.45, and 0.02 μm (Figure 1). The development of the channels was observed through optical microscopy. The obtained three layers were screwed between two acyl plates and put into a membrane. The inlet/outlet channels were connected to the syringe pump using L connectors and Tygon[®] tubing. The ethanol phase is introduced into the chip through the inlet channels of the top layer and passes through the membrane of the middle layer, finally flowing out through the outlet channel of the bottom layer.

LNP Production. The membrane pore size and continuous phase flow rate are major factors affecting LNP size.¹⁷ An eth-

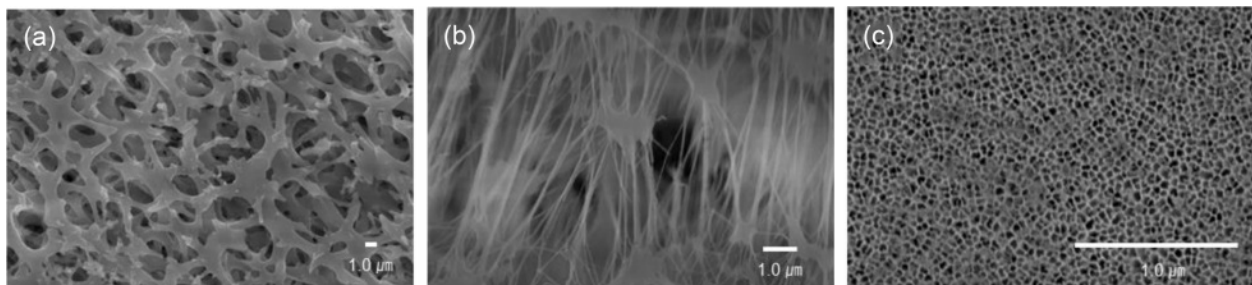


Figure 1. SEM images of the membranes with (a) 0.80 μm; (b) 0.45 μm; (c) 0.02 μm pore size.

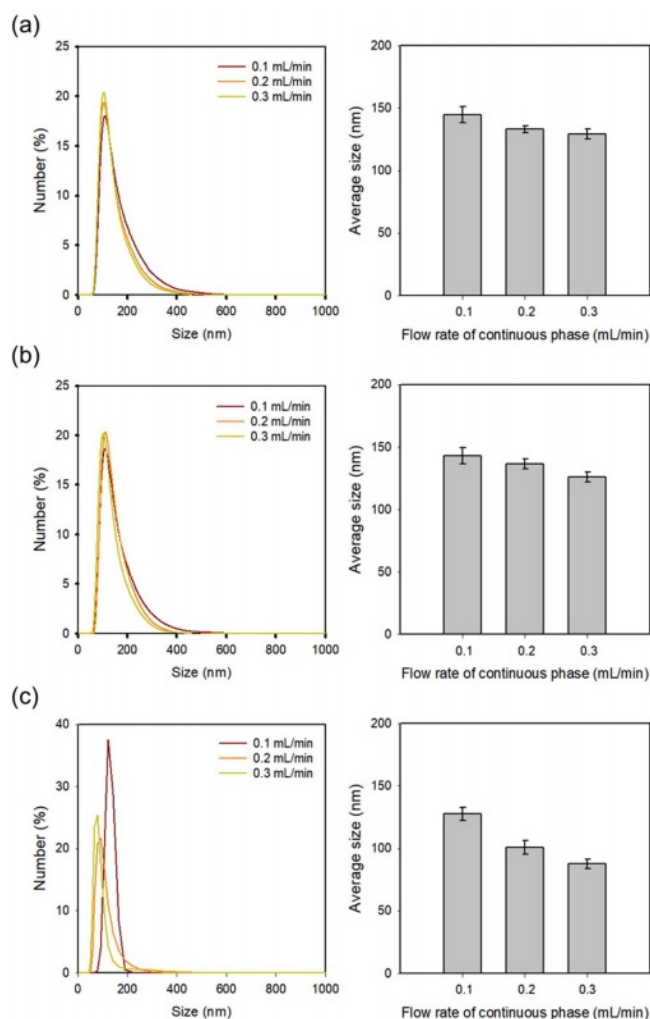


Figure 2. Size distribution and the average size of LNPs prepared by the membranes with different pore sizes of (a) 0.80 μm ; (b) 0.45 μm ; (c) 0.02 μm .

anol solution containing DPPC, cholesterol, and drugs was used for the discontinuous phase, while the water phase was used for the continuous phase. The flow rate of the continuous phase was changed to 0.1, 0.2, and 0.3 mL/min, and the flow rate of the discontinuous phase was maintained at 0.01 mL/min. Figure 2 shows the average sizes of LNPs at membrane pore diameters of 0.80, 0.45, and 0.02 μm , respectively. LNP droplets from the outlet channel were collected in a vial and gently stirred to evaporate the remaining ethanol. LNP was ultimately obtained after dialysis. When the flow rate of the continuous phase was more than 0.3 mL/min, the flow rate difference of the discontinuous phase became very large, resulting in backpressure and a low concentration of LNPs. In contrast, when the flow rate of the continuous phase was less

than 0.1 mL/min, the size of the LNP becomes too large, so measurements were performed only at flow rates of 0.1, 0.2, and 0.3 mL/min. In a 0.80 μm pore size membrane, the sizes of the LNPs were measured as 144.6 \pm 6.31, 133.1 \pm 2.70, and 129.2 \pm 3.98 nm, in a 0.45 μm pore size membrane, the size of the LNPs were measured as 142.9 \pm 6.58, 136.5 \pm 4.10, and 126.0 \pm 4.13 nm, and in a 0.02 μm pore size membrane, the size of the LNPs was measured as 127.5 \pm 5.31, 100.9 \pm 5.54, and 87.6 \pm 3.84 nm at flow rates of the continuous phase of 0.1, 0.2, and 0.3 mL/min. The reason for the significant decrease in the LNP size with the use of 0.02 μm pore size should be the much smaller pore size than the others. Their results revealed that the average size of LNPs was affected by both the membrane pore size and the flow rate of the continuous phase.¹⁷ In a 0.02 μm pore size membrane, LNPs exhibited sizes less than 100 nm, irrespective of the 0.2 mL/min and 0.3 mL/min flow rate of the continuous phase.

Drug Encapsulation. Figure 3 shows variations in the size of LNP with drugs, respectively. To evaluate the effect of drug loading, LA and DOX were used. The average LNP size increased as the drug-loaded. In the system, LA loading increased LNP size from 108.1 \pm 22.56 to 140.7 \pm 4.13 nm. Similarly, DOX loaded led to an increase in LNP size to 141.3 \pm 7.46 nm. When both were loaded, the size of LNP increased to 156.5 \pm 10.44 nm. The saturated concentration of DOX was measured as 0.26 mg/mL. In addition, the encapsulation efficiency of DOX in LNP was measured as 13.18 \pm 0.12%. This produces results comparable to encapsulation efficiency for other hydrophilic drugs.^{18,19} As the LNPs were loaded with drugs, the size of the LNPs increased. These results suggest that LNPs increased in size with drug loading. In conclusion, four types of LNPs CON, LA, DOX, and DOX-LA were prepared.

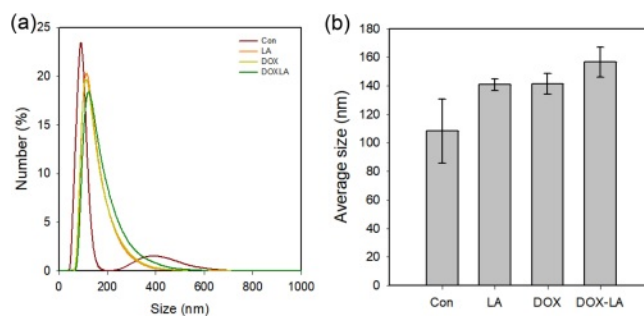


Figure 3. The size distribution and average sizes of the control, LA, DOX, and DOX-LA LNPs were prepared using 0.02 μm membrane pore size, where the flow rates of the discontinuous and continuous phases were 0.01 and 0.2 mL/min, respectively.

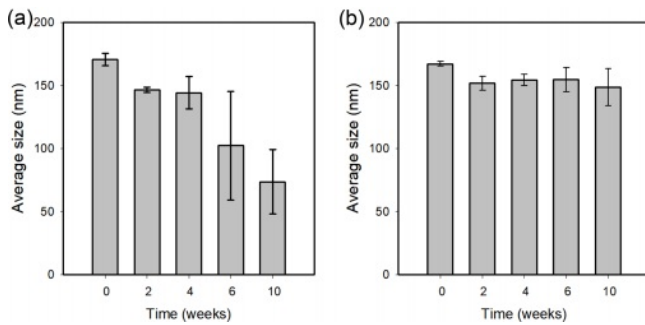


Figure 4. Variations in size of LNPs (a) without LA; (b) with LA concerning time.

Lipid Nanoparticles Stability with or Without LA. A stability study was carried out on free-drug LNPs over 10 weeks. With or without LA were selected to follow LNPs size during storage (Figure 4). LNPs without LA were unstable. The sizes of the LNPs decreased from 170.5 ± 4.86 to 73.6 ± 25.41 nm. In contrast, LNPs with LA, small differences of about a few nanometers (15–20 nm) were observed over the storage time. Figure 5 shows the morphological changes of LNP with or without LA. According to transmission electron microscope images (TEM, JEOM 1010, JEOL, Japan), LNP with LA morphology remained nearly unchanged. However, it is a distorted sphere of LNP without LA. These results suggest that LA contributes to the stability of LNP. LA has a hydrophilic portion and a hydrophobic portion and is thought to acts similarly to phospholipid to increase the stability of LNP.

In vitro Viability of LNPs with Doxorubicin and LA. The effects of LNPs on cell viability were determined using CCK assay, as shown in Figure 6. NIH-3T3 and HeLa cell lines were chosen for in vitro experiments as model cells. Considering the encapsulation efficiency of the LNP-DOX, the same amount of DOX (free drug) was added to both the cell lines. In addition, the cells were treated with three types of LNP-LA, LNP-DOX, and LNP-DOX-LA where the number of the nanoparticles was adjusted to the same (8.76×10^{11} par-

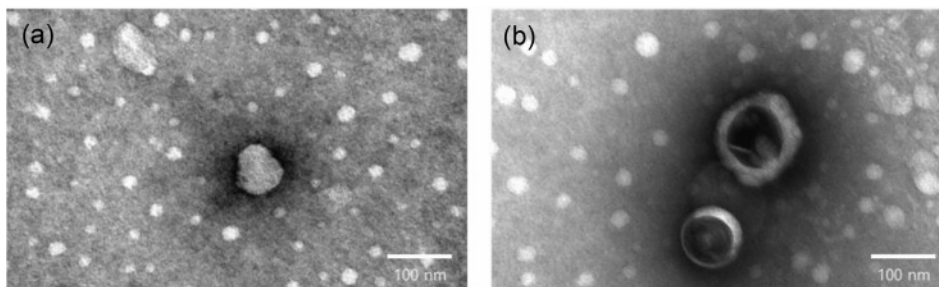


Figure 5. TEM images of LNPs (a) without LA; (b) with LA.

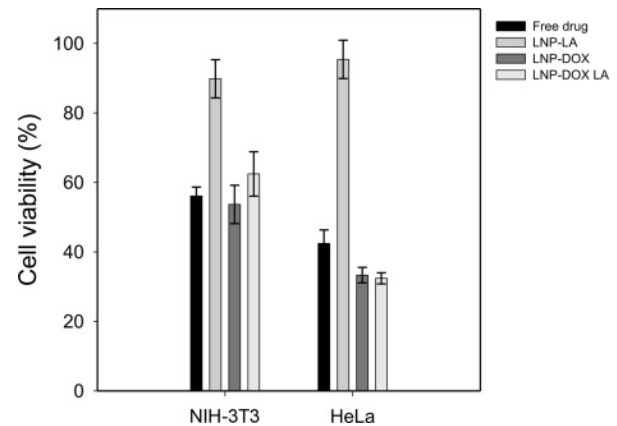


Figure 6. Viability of NIH3T3 and HeLa cell lines after the addition of LNP dispersions with the concentration of 8.76×10^{11} particles/mL.

ticles/mL). In the case of LNP-LA, there was no significant difference in the viability of the cells, suggesting a little effect of LA on cell viability. The presence of LA enhanced the LNP stability, as presented in Figure 4. As for NIH-3T3, there was a little difference in the cell viability after treatments of free drug, LNP-DOX, and LNP-DOX-LA. However, the LNP-DOX exhibited lower viability of HeLa than the free drug group. These results confirmed the enhanced toxicity of the LNP-DOX for HeLa cells.^{20,21}

Conclusions

In conclusion, the microfluidic device with a porous membrane was prepared for the continuous production of LNPs. The procedure for the device fabrication was simple and required no expensive equipment. The smaller LNPs were prepared at the higher flow rate of the continuous phase by using a membrane with smaller pore size. In the continuous phase, the flow rate and shear stress of the pores influence the size of the LNP. The smaller the pore size and the faster the continuous phase flow rate, the smaller the LNP. The LNP with

LA exhibited enhanced colloidal stability. In vitro test revealed that the LNPs with doxorubicin and lauric acid exhibited lower viability for HeLa cells than NIH3T3 cells. Our approach can be utilized as a platform technology for the generation of various LNPs with active agents such as drugs, DNA, and RNA.

Acknowledgments: This study was supported by the National Research Foundation of Korea (NRF) grant funded by the Korean government (MIST) (No. 2021R1A2C1003865) and Korea Drug Development Fund funded by the Ministry of Science and ICT, Ministry of Trade, Industry, and Energy, and Ministry of Health and Welfare (HN21C0317, Republic of Korea), the Korea Medical Device Development Fund grant funded by the Korea government (the Ministry of Science and ICT, the Ministry of Trade, Industry and Energy, the Ministry of Health & Welfare, the Ministry of Food and Drug Safety) (202012D21-02), and the Research Fund, 2022 of The Catholic University of Korea.

Conflict of Interest: The authors declare that there is no conflict of interest.

References

- Kraft, J. C.; Freeling, J. P.; Wang, Z.; Ho, R. J. Emerging Research and Clinical Development Trends of Liposome and Lipid Nanoparticle Drug Delivery Systems. *J. Pharm. Sci.* **2014**, *103*, 29-52.
- Souto, E. B.; Doktorová, S. Solid Lipid Nanoparticle Formulations: Pharmacokinetic and Biopharmaceutical Aspects in Drug Delivery. *Methods. Enzymol.* **2009**, *464*, 105-129.
- Fenton, O. S.; Kauffman, K. J.; McClellan, R. L.; Kaczmarek, J. C.; Zeng, M. D.; Andresen, J. L.; Rhym, L. H.; Heartlein, M. W.; DeRosa, F.; Anderson, D. G. Customizable Lipid Nanoparticle Materials for the Delivery of siRNAs and mRNAs. *Angew. Chem. Int. Ed. Engl.* **2018**, *57*, 13582-13586.
- Eygeris, Y.; Patel, S.; Jozic, A.; Sahay, G. Deconvoluting Lipid Nanoparticle Structure for Messenger RNA Delivery. *Nano Lett.* **2020**, *20*, 4543-4549.
- Pizzol, C. D.; Filippin-Monteiro, F. B.; Restrepo, J. A.; Pittella, F.; Silva, A. H.; Alves de Souza, P.; Machado de Campos, A.; Creczynski-Pasa, T. B. Influence of Surfactant and Lipid Type on the Physicochemical Properties and Biocompatibility of Solid Lipid Nanoparticles. *Int. J. Environ. Res. Public Health* **2014**, *11*, 8581-8596.
- Wang, L.; Li, H.; Wang, S.; Liu, R.; Wu, Z.; Wang, C.; Wang, Y.; Chen, M. Enhancing the Antitumor Activity of Berberine Hydrochloride by Solid Lipid Nanoparticle Encapsulation. *AAPS. PharmSciTech.* **2014**, *15*, 834-844.
- Gkeka, P.; Sarkisov, L.; Angelikopoulos, P. Homogeneous Hydrophobic-Hydrophilic Surface Patterns Enhance Permeation of Nanoparticles through Lipid Membranes. *J. Phys. Chem. Lett.* **2013**, *4*, 1907-1912.
- Patel, D.; Kumar, V.; Kesharwani, R.; Mazumdar, B. Lipid Nanoparticle a Novel Carrier for Cosmetics and Topical Preparation: A Review. *Inven. Rapid Cosmeceuticals* **2015**, *3*, 1-6.
- Shu, L.; Fu, F.; Huang, Z.; Huang, Y.; Hu, P.; Pan, X. Nanostructure of DiR-Loaded Solid Lipid Nanoparticles with Potential Bioimaging Functions. *AAPS. PharmSciTech.* **2020**, *21*, 321.
- Monteiro, N.; Martins, A.; Reis, R. L.; Neves, N. M. Liposomes in Tissue Engineering and Regenerative Medicine. *J. R. Soc. Interface* **2014**, *11*, 20140459.
- Liu, X.; Bahloul, B.; Lai Kuen, R.; Andrieux, K.; Roques, C.; Scherman, D. Cationic Lipid Nanoparticle Production by Microfluidization for siRNA Delivery. *Int. J. Pharm.* **2021**, *605*, 120772.
- De Jesus, M. B.; Radaic, A.; Zuhorn, I. S.; de Paula, E. Microemulsion Extrusion Technique: a New Method to Produce Lipid Nanoparticles. *J. Nanopart. Res.* **2013**, *15*, 1960.
- Shepherd, S. J.; Warzecha, C. C.; Yadavali, S.; El-Mayta, R.; Alameh, M. G.; Wang, L.; Weissman, D.; Wilson, J. M.; Issadore, D.; Mitchell, M. J. Scalable mRNA and siRNA Lipid Nanoparticle Production Using a Parallelized Microfluidic Device. *Nano Lett.* **2021**, *21*, 5671-5680.
- Ren, K.; Zhou, J.; Wu, H. Materials for Microfluidic Chip Fabrication. *Acc. Chem. Res.* **2012**, *46*, 2396-2406.
- Xia, Y.; Whitesides, G. M. Soft Lithography, *Annu. Rev. Mater. Res.* **1998**, *28*, 153-184.
- Qin, D.; Xia, Y.; Whitesides, G. M. Soft Lithography for Micro- and Nanoscale Patterning. *Nat. Protoc.* **2010**, *5*, 491-502.
- Charcosset, C.; Limayem, I.; Fessi, H. The Membrane Emulsification Process – A Review. *J. Chem. Technol. Biotechnol.* **2004**, *79*, 209-218.
- Berger, N.; Sachse, A.; Bender, J.; Schubert, R.; Brandl, M. Filter Extrusion of Liposomes Using Different Devices: Comparison of Liposome Size, Encapsulation Efficiency, and Process Characteristics. *Int. J. Pharm.* **2001**, *223*, 55-68.
- Nii, T.; Ishii, F. Encapsulation Efficiency of Water-soluble and Insoluble Drugs in Liposomes Prepared by the Microencapsulation Vesicle Method. *Int. J. Pharm.* **2005**, *298*, 198-205.
- Barraud, L.; Merle, P.; Soma, E.; Lefrançois, L.; Guerret, S.; Chevallier, M.; Dubernet, C.; Couvreur, P.; Treppe, C.; Vitvitski, L. Increase of Doxorubicin Sensitivity by Doxorubicin-loading into Nanoparticles for Hepatocellular Carcinoma Cells *in vitro* and *in vivo*. *J. Hepatol.* **2005**, *42*, 736-743.
- Tong, N.; Zhang, J.; Chen, Y.; Li, Z.; Luo, Y.; Zuo, H.; Zhao, X. Berberine Sensitizes Multiple Human Cancer Cells to the Anticancer Effects of Doxorubicin *in vitro*. *Oncol. Lett.* **2012**, *3*, 1263-1267.

Publisher's Note The Polymer Society of Korea remains neutral with regard to jurisdictional claims in published articles and institutional affiliations.